Magn Reson Med Sci, Vol. 14, No. 1, pp. 43–50, 2015 doi:10.2463/mrms.2014-0024

MAJOR PAPER

Diffusion-weighted Line-scan Echo-planar Spectroscopic Imaging Technique to Reduce Motion Artifacts in Metabolite Diffusion Imaging

Yoshitaka Bito[1,2,3]*, Koji Hirata[1], Toshihiko Ebisu[4], Yuko Kawai[5], Yosuke Otake[1], Satoshi Hirata[1], Toru Shirai[1], Yoshihisa Soutome[1], Hisaaki Ochi[1], Etsuji Yamamoto[3], Masahiro Umeda[5], Toshihiro Higuchi[6], and Chuzo Tanaka[6]

[1]*Central Research Laboratory, Hitachi, Ltd.*
[2]*MRI System Division, Hitachi Medical Corporation*
2–1 Shintoyofuta, Kashiwa-shi, Chiba 277–0804, Japan
[3]*Faculty of Engineering, Graduate School of Engineering, Chiba University*
[4]*Department of Neurosurgery, Nantan General Hospital*
[5]*Department of Medical Informatics, Meiji University of Integrative Medicine*
[6]*Department of Neurosurgery, Meiji University of Integrative Medicine*
(Received February 24, 2014; Accepted May 28, 2014; published online October 27, 2014)

Metabolite diffusion is expected to provide more specific microstructural and functional information than water diffusion. However, highly accurate measurement techniques have still not been developed, especially for reducing motion artifacts caused by cardiac pulsation and respiration. We developed a diffusion-weighted line-scan echo-planar spectroscopic imaging (DW-LSEPSI) technique to reduce such motion artifacts in measuring diffusion-weighted images (DWI) of metabolites. Our technique uses line-scan and echo-planar techniques to reduce phase errors induced by such motion during diffusion time. The phase errors are corrected using residual water signals in water suppression for each acquisition and at each spatial pixel specified by combining the line-scan and echo-planar techniques. We apply this technique to a moving phantom and a rat brain *in vivo* to demonstrate the reduction of motion artifacts in DWI and apparent diffusion coefficient (ADC) maps of metabolites. DW-LSEPSI will be useful for investigating a cellular diffusion environment using metabolites as probes.

Keywords: ***diffusion*, *metabolite*, *motion artifact*, *rat*, *spectroscopic imaging***

Introduction

Metabolite diffusion is expected to provide useful information regarding cellular and tissue microstructures and functions, such as cell size, permeability, and intracellular transport.[1–4] Many studies have used diffusion-weighted spectroscopy (DWS) especially to investigate changes in metabolite diffusion at ischemia[5–9] and properties of metabolite diffusion that differ from those of water.[10–15] However, only a few studies have employed diffusion-weighted spectroscopic imaging (DWSI).[16–18] One reason is that an efficient measurement technique has not been developed to obtain highly accurate diffusion-weighted images (DWI) of metabolites. The issues in developing the technique are low signal-to-noise ratio (SNR), long measurement time, low spatial resolution, and artifacts caused by magnetic field inhomogeneity. However, the most challenging issue is to reduce motion artifacts caused by cardiac pulsation or respiration.[17] Such motion during diffusion time induces an imbalance of the diffusion gradients that causes phase errors. The phase errors become much larger when larger *b*-values are used for the accurate detection of diffusion of metabolites that is smaller than diffusion of water. The large phase errors hinder accurate phase-

*Corresponding author, Phone: +81-4-7131-3221, Fax: +81-4-7134-1170, E-mail: yoshitaka.bito.dn@hitachi.com

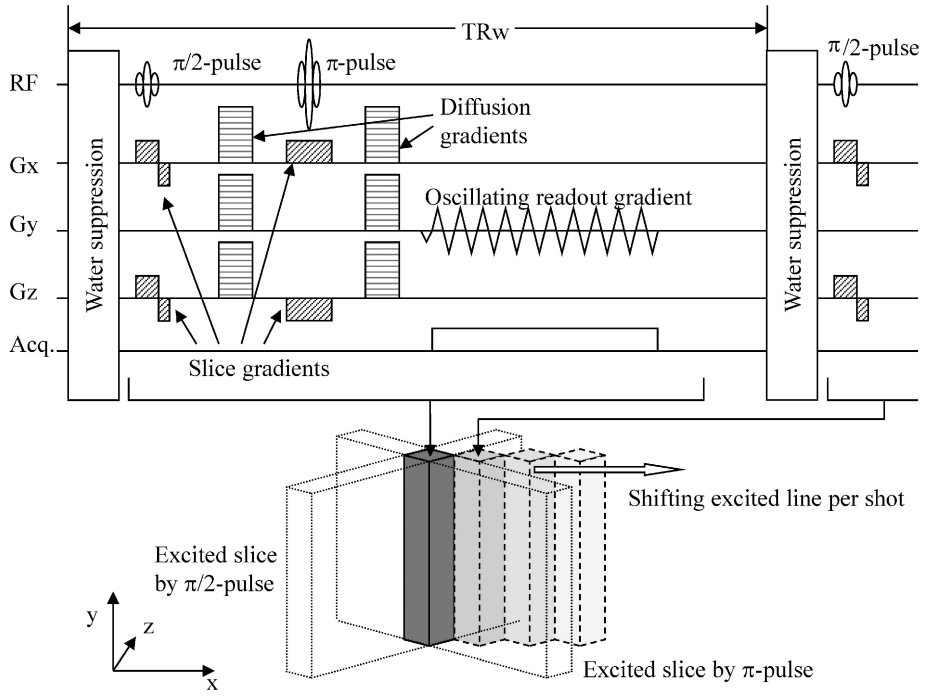

Fig. 1. A schematic diagram of sequence and an excited line of our diffusion-weighted line-scan echo-planar spectroscopic imaging (DW-LSEPSI) technique. The excited line by $\pi/2$-pulse and π-pulse is shifted shot-by-shot at a repetition time (TRw) to acquire spatial information in the x-direction. An oscillating readout gradient is used for the simultaneous acquisition of spatial information in the y-direction and chemical shift information.

encoding and produce ghosting artifacts in imaging. Furthermore, they hinder accurate amplitude summation and cause significant signal loss artifact in signal averaging which is necessary to mitigate the low SNR of metabolite signals. These phase errors depend on spatial location and vary with time, so they are significantly difficult to correct using conventional phase-encoding. Thus, such motion artifacts have not been effectively reduced using proposed diffusion-weighted chemical-shift imaging with 2-dimensional phase-encoding and navigator echo[17] and diffusion-weighted echo-planar spectroscopic imaging (DW-EPSI) that uses echo-planar and one-dimensional phase-encoding.[18] Diffusion-weighted line-scan echo-planar spectroscopic imaging (DW-LSEPSI), which uses echo-planar and line-scan techniques instead of phase-encoding, has been proposed to reduce such motion artifacts and tested by measuring a water phantom but not by measuring metabolite signal *in vivo*.[19]

We have developed a DW-LSEPSI technique for the accurate imaging of metabolite diffusion *in vivo*. Because there is no phase-encoding, there is no ghosting artifact. The combination of line-scan and echo-planar techniques can specify the location of all pixels on the line for each acquisition to enable correction of phase errors at each spatial pixel in signal averaging. We applied DW-LSEPSI to a moving phantom and to a rat brain *in vivo* to acquire diffusion-weighted images and apparent diffusion coefficient (ADC) maps of metabolites. Preliminary reports of this work have been presented.[20,21]

Materials and Methods

Diffusion-weighted line-scan echo-planar spectroscopic imaging (DW-LSEPSI)

The DW-LSEPSI method we developed uses line-scan and echo-planar techniques to acquire spatial and spectral information and diffusion gradients to add diffusion information (Fig. 1). The region excited by the $\pi/2$- and π-pulses, having a diamond-shaped cross-section, is shifted diagonally, i.e., along the x-direction, shot-by-shot in a short time, which maximizes the SNR per measurement time up to half the SNR using normal slice selection.[22] The reason is that this line-scan technique excites up to half the volume of the slice excited by the normal slice selection in repetition time (TR) like multislice technique. The oscillating readout gradient is used to acquire data along the sinusoidal tra-

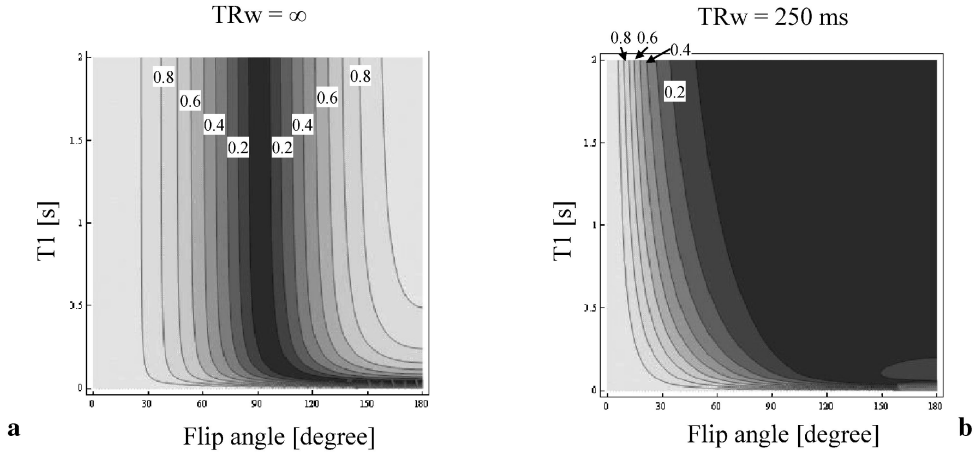

Fig. 2. Contour maps of the rate of water suppression relative to the T_1 and flip angle values for the cases of (**a**) TRw = ∞ and (**b**) TRw = 250 ms, where TRw is the repetition time of the line-scan shot. The suppression rate differs significantly between b and a.

jectory in the ky-time space.[18] The acquired data is reordered in the ky-time space and is inverse Fourier transformed to obtain both the spatial information in the y-direction and chemical shift information simultaneously. Thus, the spatial locations of acquired pixels can be specified for each shot. A single Gaussian radiofrequency (RF) pulse is used for water suppression to reduce the duration of the line-scan shot. Although conventional spectroscopy/spectroscopic imaging uses multiple Gaussian RF pulses to suppress the water signal efficiently at a wide range of T_1 and flip angle of transmitted RF pulses, a single Gaussian RF pulse is efficient for LSEPSI because the short repetition time of the water suppression pulses (TRw) makes a series of single pulses comparable to multiple pulses. Figure 2 compares suppression rates at TRw = ∞ and TRw = 250 ms. Shorter repetition time improves the suppression rate at a wide range of T_1 and flip angle.[21] The amplitude of the RF pulse for water suppression is adjusted to retain the water signal for phase correction depending on the duration of the line-scan shot and diffusion weighting. Signal averaging is performed along with phase correction, and the amount of phase correction is calculated to equalize the phase of the residual water signal at each pixel. This mitigates the signal loss induced by phase errors caused by motion.

Experiments: moving phantom and rat brain in vivo

We used a 7-tesla MR imaging unit for small animal study (Agilent Technologies, Inc., USA) equipped with actively shielded gradient coils of 120-mm inner diameter capable of producing a maximum amplitude of 400 mT/m within 150 µs, linear birdcage resonator of 70-mm diameter for RF transmission/receive and 2-channel surface coil tuned to rat brains for RF receive (Rapid Biomedical, Inc., Germany).

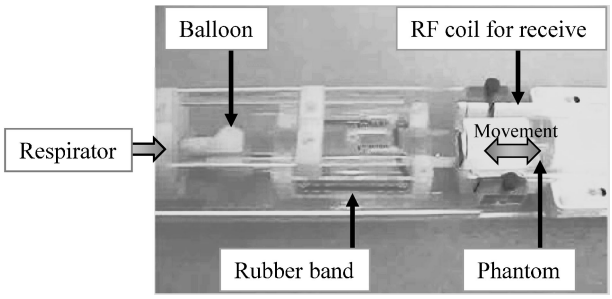

Fig. 3. A moving phantom driven by a respirator. We used a respirator to inflate a small balloon to move the phantom to the right and a rubber band to return the phantom to the left when the balloon was deflated.

To demonstrate the effectiveness of DW-LSEPSI in reducing motion artifacts, we used a moving phantom and a rat brain *in vivo*. The phantom was a glass bottle of 20-mm inner diameter filled with 100-mM of N-acetylaspartate (NAA) solution at 24°C. We oscillated the phantom at 110 cycles/min for a length of 0.3 mm along the z-direction driven by tensing a rubber band and inflating a small balloon using a respirator (Fig. 3). We chose the cycle in a higher range of normal respiratory rate not to synchronize with the used TR of 4000 ms described later to enlarge the signal loss by motion. We chose the length to represent visualization of the motion of the loosely fixed rat head. In this phantom experiment, the birdcage resonator was used both for RF transmit and receive.

We employed a male 280-g Wistar rat for *in vivo* study, fixing the rat's head at 3 points (foreteeth

and both earholes) in a dorsal state using a plastic bar attached on the surface coil. The rectal temperature was maintained between 37.5 and 38.5°C using a warm-water blanket. A mixture of isoflurane and room air was sent by a respirator to the rat head for anesthesia. Remarkably, this experiment was done under free breathing conditions with no tracheal intubation and no gating which easily causes large motion artifacts in conventional DWSI. This rat experiment utilized the birdcage resonator for RF transmit and the surface coil for RF receive.

We compared DW-LSEPSI with DW-EPSI,[18] which uses phase-encoding instead of line-scanning in the x-direction. The measurement parameters for both techniques were: TR, 4000 ms; echo time (TE), 136 ms; spectral bandwidth, 7.24 ppm (128 points); field of vision (FOV) in y, 40 mm (16 pixels); and slice thickness, 2.5 mm. FOV in x was 40 mm (16 encodes) for DW-EPSI and 30 mm (12 lines) for DW-LSEPSI, which equalized their spatial resolutions at 2.5 mm. To equalize the measurement times of both techniques, we utilized numbers of averaging for the phantom experiment were 1 for DW-EPSI and 16 for DW-LSEPSI, and those for the rat brain experiment were 8 for DW-EPSI and 128 for DW-LSEPSI. Diffusion gradients were added in the z-direction, of which duration and interval $\delta/\Delta = 6/62$ ms. We used b-values of 0, 550, 1090, and 1700×10^6 s/m^2 for the phantom experiment and 0, 550, 1700, and 3030×10^6 s/m^2 for the rat brain experiment. The total measurement times of both techniques were the same, about 4 min for the phantom experiment and 34 min for the brain experiment. DWIs of water and NAA were calculated by cut and sum of the signals along corresponding chemical shift regions for all measurements. We calculated ADC maps of water and NAA by fitting the DWIs to a single exponential decay along the b-value only for DW-LSEPSI because DWIs showed large motion artifacts in DW-EPSI.

Results and Discussion

Figure 4 shows spectroscopic images of the phantom obtained by both DW-EPSI and DW-LSEPSI. In each spectroscopic image, the graph represents the spectra integrated in the whole spatial region. The x-axis is the chemical shift ranging from 6.24 to −1.00 ppm for every graph, and the y-axis is signal intensity normalized by peak water signal for the graphs of non-water suppression, and the y-axis is normalized by a certain value for the graphs of water suppression for easy visualization of the signal decay of NAA with the b-value. The image was calculated by integrating the signal in the selected region of chemical shift shown as a dashed line in the graph. As shown in Figure 4, good spectroscopic images of the phantom were obtained by both DW-EPSI and DW-LSEPSI at $b = 0$. Ghosting artifact and signal loss are evident in DW-EPSI when b is larger than 0, but no such artifacts can be seen in DW-LSEPSI. Figure 5 shows spectroscopic images of the rat brain *in vivo*. In each spectroscopic image, the graph represents the spectra obtained from the selected brain region shown as a white dashed rectangle, and the image was calculated by integrating the signal in the selected chemical shift region shown as a dashed line. The white solid lines represent the calculated outline of the rat head using T_1-weighted image. Similarly for the phantom result, motion artifacts can be seen in DW-EPSI but not in DW-LSEPSI when b is larger than 0. ADC maps of NAA were calculated for both the phantom and rat brain using DW-LSEPSI but not using DW-EPSI because of the severe motion artifacts (Fig. 6). They show successfully calculated ADC maps, but the maps show slight spatial variance. This variance may result from the diffusion property of NAA and/or measurement error by using DW-LSEPSI. Addition of the diffusion gradient in only the z-direction may cause the ADC of NAA to become smaller in the radial axon near the cortex than in other regions, and insufficient phase correction near the base at larger b-values as a result of the smaller SNR near the base using the surface coil may cause the ADC of NAA to become larger near the base than in other regions. Motion may also be larger near the base from free breathing than that near the cortex because the rat head was fixed on the surface coil in the dorsal state.

As shown in Table, the calculated ADCs in the moving phantom at 24°C using DW-LSEPSI were $2.35 \pm 0.15 \times 10^{-9}$ m^2/s for water and $0.72 \pm 0.04 \times 10^{-9}$ m^2/s for NAA, which agree well with previously reported values obtained at 20°C using DWS $2.00 \pm 0.05 \times 10^{-9}$ m^2/s (water) and $0.85 \pm 0.05 \times 10^{-9}$ m^2/s (NAA)[2] and $2.15 \pm 0.04 \times 10^{-9}$ m^2/s (water) and $0.61 \pm 0.06 \times 10^{-9}$ m^2/s (NAA).[6] The higher ADC of water in our results is attributable mainly to the temperature dependence of the ADC, which is estimated to be about 0.23×10^{-9} m^2/s between 24 and 20°C.[23] This result demonstrates the improved accuracy in ADC measurement by the reduction of motion artifacts using DW-LSEPSI. The calculated ADC of NAA in the rat brain *in vivo* using DW-LSEPSI was $0.34 \pm 0.04 \times 10^{-9}$ m^2/s, which seems higher than reported values $0.27 \pm 0.04 \times 10^{-9}$ m^2/s^2 and $0.17 \pm 0.04 \times 10^{-9}$ m^2/s.[6] This may be explained by insufficient reduction of motion artifact at higher b-val-

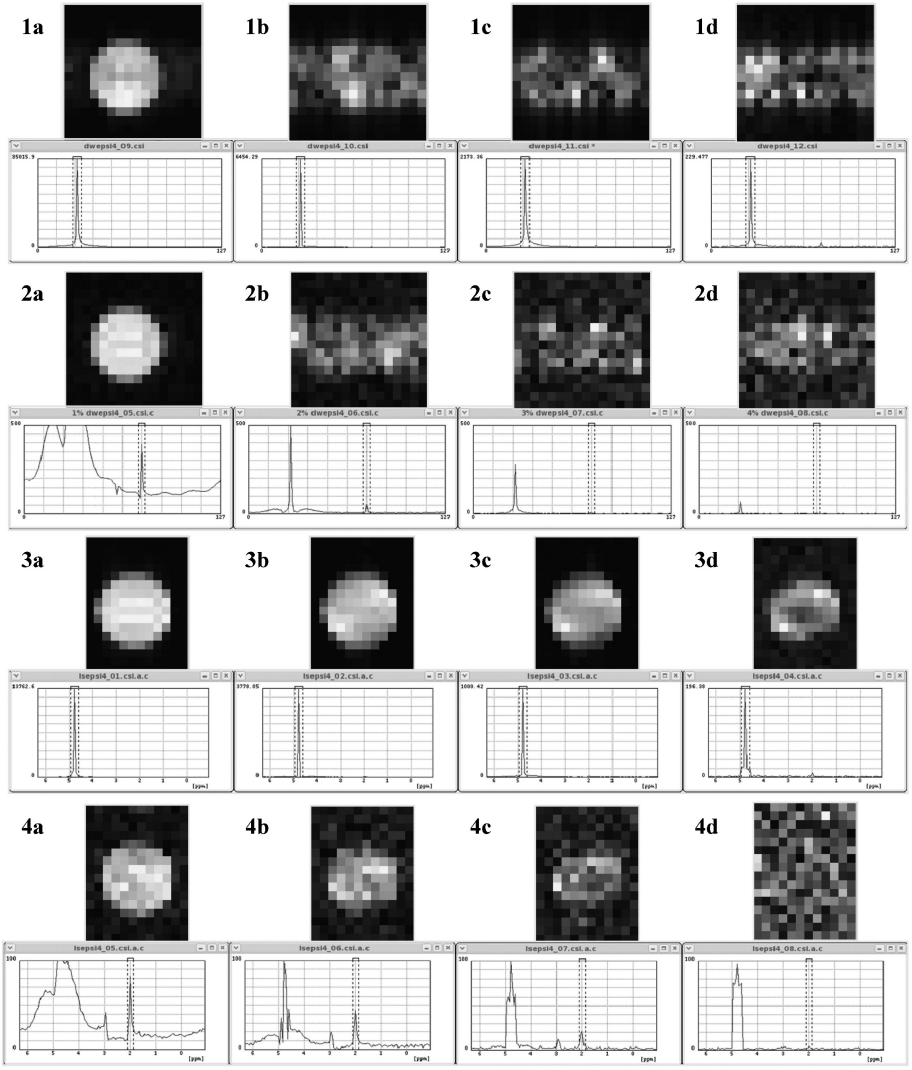

Fig. 4. Diffusion-weighted spectroscopic images of a moving phantom. 1. Water images obtained using diffusion-weighted echo-planar spectroscopic imaging (DW-EPSI) without water suppression. 2. N-acetylaspartate (NAA) images obtained by DW-EPSI with water suppression. 3. Water images obtained using diffusion-weighted line-scan echo-planar spectroscopic imaging (DW-LSEPSI) without water suppression. 4. NAA images obtained using DW-LSEPSI with water suppression. In each image, *b*-values are: a, 0; b, 550; c, 1090; and d, 1700 ($\times 10^6$ s/m^2).

ues using DW-LSEPSI, acquisition of regions by DWSI that are not acquired by DWS, and/or diffusion properties of NAA. The interesting diffusion properties of NAA are non-monoexponential decay along with *b*-values and dependency with diffusion time[10–12] and higher diffusion anisotropy.[13–15] These diffusion properties of metabolites should be investigated further.

Other methods proposed to reduce motion artifacts are diffusion-weighted echo-planar spectroscopic imaging with a pair of bipolar diffusion gradients (DW-EPSI with BPGs)[24] and diffusion-sensitive single-shot proton-echo-planar-spectroscopic imaging (DW-SS-PEPSI).[25] DW-EPSI with BPGs uses a pair of bipolar diffusion gradients to reduce the phase error caused by uniform motion. DW-LSEPSI has an advantage over DW-EPSI with BPGs in non-uniform motion but a disadvantage in non-rigid motion, such as inflating motion. It may be better to select DW-LSEPSI or DW-EPSI with BPGs in accordance with the target motion. DW-SS-PEPSI uses 2-dimensional echo-planar and parallel imaging to acquire whole data in a single-shot. DW-SS-PEPSI may better reduce motion artifacts, but quality of acquired data is limited, perhaps as a result of the high frequency oscillating gradient and reduced SNR in parallel imaging.

DW-LSEPSI also has a disadvantage in SNR per

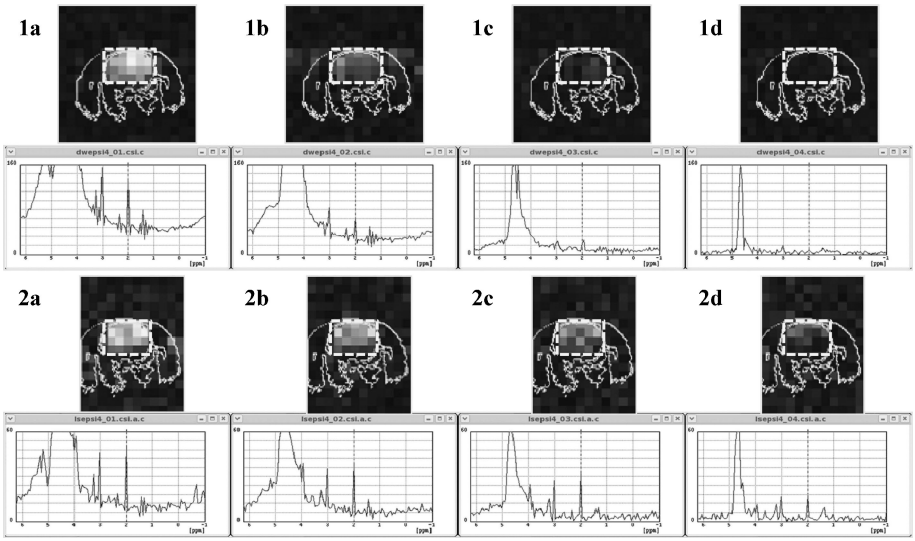

Fig. 5. Diffusion-weighted spectroscopic images of a rat brain. 1. N-acetylaspartate (NAA) images obtained using diffusion-weighted echo-planar spectroscopic imaging (DW-EPSI) with water suppression. 2. NAA images obtained using diffusion-weighted line-scan echo-planar spectroscopic imaging (DW-LSEPSI) with water suppression. In each image, *b*-values are: a, 0; b, 550; c, 1700; and d, 3030 ($\times 10^6$ s/m^2).

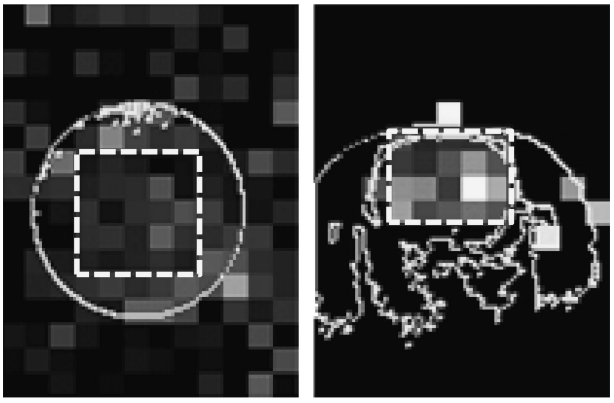

Fig. 6. Calculated apparent diffusion coefficient (ADC) maps of N-acetylaspartate (NAA) in (**a**) a moving phantom and (**b**) a rat brain *in vivo* obtained using diffusion-weighted line-scan echo-planar spectroscopic imaging (DW-LSEPSI). The white dashed rectangles represent the regions in which average and standard deviation were calculated. The white solid lines represent the outlines of the phantom and the rat head.

Table. Calculated ADC of NAA and water in a phantom and a rat brain by using DW-LSEPSI

	ADC (mean ± standard deviation) (10^{-9} m^2/s)	
	NAA	Water
Phantom (24°C)	0.72 ± 0.04	2.35 ± 0.15
Rat brain	0.34 ± 0.04	—

measurement time because the excited line has a diamond-shaped cross-section, and the excited volume is up to half of the normal slice selection. The calculated SNR of DW-LSEPSI was 30% of that of DW-EPSI for the moving phantom at $b = 0$. Although this SNR reduction is mostly a tradeoff for improved spatial resolution in both the x- and z-directions, loss at the edge of slicing becomes larger when the spatial resolution becomes smaller. Improved SNR requires an excitation pulse with better slice profile. SNR may also be improved using a parallel line scan, which uses parallel excitation of multiple lines simultaneously and parallel imaging to identify excited each line.[26,27] Using this technique, SNR can be increased along with the ratio of the number of excited lines to a geometric factor.

DW-LSEPSI requires further improvements to overcome its disadvantages, but our results suggest it will be a useful technique for investigating spatial information about metabolite diffusion *in vivo*.

Conclusion

We developed a DW-LSEPSI technique that combines line-scan and echo-planar techniques to obtain accurate diffusion-weighted images and ADC maps of metabolites by reducing motion artifacts, and we compared it with conventional DW-EPSI in experiments with a moving phantom and a rat brain

in vivo. Our results demonstrate that the developed DW-LSEPSI efficiently reduces motion artifacts. DW-LSEPSI will be a powerful tool for studies of diffusion images of metabolites in both basic science and clinical use.

References

1. Moonen CT, van Zijl PC, Le Bihan D, DesPres D. *In vivo* NMR diffusion spectroscopy: ^{31}P application to phosphorus metabolites in muscle. Magn Reson Med 1990; 13:467–477.
2. Merboldt KD, Hörstermann D, Hänicke W, Bruhn H, Frahm J. Molecular self-diffusion of intracellular metabolites in rat brain *in vivo* investigated by localized proton NMR diffusion spectroscopy. Magn Reson Med 1993; 29:125–129.
3. Posse S, Cuenod CA, Le Bihan D. Human brain: proton diffusion MR spectroscopy. Radiology 1993; 188:719–725.
4. Nicolay K, Braun KP, Graaf RA, Dijkhuizen RM, Kruiskamp MJ. Diffusion NMR spectroscopy. NMR Biomed 2001; 14:94–111.
5. Wick M, Nagatomo Y, Prielmeier F, Frahm J. Alteration of intracellular metabolite diffusion in rat brain *in vivo* during ischemia and reperfusion. Stroke 1995; 26:1930–1933.
6. van der Toorn A, Dijkhuizen RM, Tulleken CA, Nicolay K. Diffusion of metabolites in normal and ischemic rat brain measured by localized ^{1}H MRS. Magn Reson Med 1996; 36:914–922.
7. Abe O, Okubo T, Hayashi N, et al. Temporal changes of the apparent diffusion coefficients of water and metabolites in rats with hemispheric infarction: experimental study of transhemispheric diaschisis in the contralateral hemisphere at 7 tesla. J Cereb Blood Flow Metab 2000; 20:726–735.
8. Dreher W, Busch E, Leibfritz D. Changes in apparent diffusion coefficients of metabolites in rat brain after middle cerebral artery occlusion measured by proton magnetic resonance spectroscopy. Magn Reson Med 2001; 45:383–389.
9. Harada M, Uno M, Hong F, Hisaoka S, Nishitani H, Matsuda T. Diffusion-weighted *in vivo* localized proton MR spectroscopy of human cerebral ischemia and tumor. NMR Biomed 2002; 15:69–74.
10. Assaf Y, Cohen Y. *In vivo* and *in vitro* bi-exponential diffusion of N-acetyl aspartate (NAA) in rat brain: a potential structural probe? NMR Biomed 1998; 11: 67–74.
11. Assaf Y, Cohen Y. Non-mono-exponential attenuation of water and N-acetyl aspartate signals due to diffusion in brain tissue. J Magn Reson 1998; 131: 69–85.
12. Kroenke CD, Ackerman JJ, Yablonskiy DA. On the nature of the NAA diffusion attenuated MR signal in the central nervous system. Magn Reson Med 2004; 52:1052–1059.
13. Ellegood J, Hanstock CC, Beaulieu C. Diffusion tensor spectroscopy (DTS) of human brain. Magn Reson Med 2006; 55:1–8.
14. Ellegood J, McKay RT, Hanstock CC, Beaulieu C. Anisotropic diffusion of metabolites in peripheral nerve using diffusion weighted magnetic resonance spectroscopy at ultra-high field. J Magn Reson 2007; 184:20–28.
15. Upadhyay J, Hallock K, Erb K, Kim DS, Ronen I. Diffusion properties of NAA in human corpus callosum as studied with diffusion tensor spectroscopy. Magn Reson Med 2007; 58:1045–1053.
16. Xin M, Ng TC, Modic M. Reverse alternations of diffusion-weighted metabolites detected in human brain tumors and in the contralateral normals using proton chemical shift imaging. In: Proceedings of the 12th Annual Meeting of SMRM, New York, USA, 1993; 68.
17. Posse S, Cuenod CA, Le Bihan D. Motion artifact compensation in ^{1}H spectroscopic imaging by signal tracking. J Magn Reson 1993; B102:222–227.
18. Bito Y, Hirata S, Nabeshima T, Yamamoto E. Echo-planar diffusion spectroscopic imaging. Magn Reson Med 1995; 33:69–73.
19. Bito Y, Hirata S, Tsukada K. Echo-planar diffusion spectroscopic imaging: reduction of motion artifacts using line-scan technique. In: Proceedings of the 6th Annual Meeting of ISMRM, Sydney, Australia, 1998; 1235.
20. Bito Y, Hirata K, Ebisu T, et al. Diffusion-weighted line-scan echo-planar spectroscopic imaging for improved accuracy in metabolite diffusion imaging. In: Proceedings of the 17th Annual Meeting of ISMRM, Hawaii, USA 2009; 334.
21. Bito Y, Hirata K, Ebisu T, et al. Water suppression for diffusion-weighted line-scan echo-planar spectroscopic imaging. In: Proceedings of the 18th Annual Meeting of the International Society for Magnetic Resonance Imaging, Stockholm, Sweden, 2010; 959.
22. Oshio K, Kyriakos W, Mulkern RV. Line scan echo planar spectroscopic imaging. Magn Reson Med 2000; 44:521–524.
23. Tofts PS, Lloyd D, Clark CA, et al. Test liquids for quantitative MRI measurements of self-diffusion coefficient *in vivo*. Magn Reson Med 2000; 43:368–374.
24. Bito Y, Hirata K, Ebisu T, et al. Motion artifact reduction using bipolar diffusion gradients in diffusion-weighted echo-planar spectroscopic imaging. In: Proceedings of the 18th Annual Meeting of the International Society for Magnetic Resonance Imaging, Stockholm, Sweden, 2010; 24.
25. Posse S, Yoshimoto AE, Otazo R, van der Kouwe A, Lin FH, Wald LL. Diffusion-sensitive single-shot proton-echo-planar-spectroscopic-imaging (PEPSI) in human brain. In: Proceedings of the 17th Annual Meeting of ISMRM, Hawaii, USA, 2009; 3521.
26. Chu R, Madore B, Panych LP, Maier S. Parallel line scan diffusion imaging. In: Proceedings of the 16th

Annual Meeting of ISMRM, Toronto, Canada, 2008; 761.
27. Bito Y, Shirai T, Hirata S, et al. Parallel line-scan echo-planar spectroscopic imaging. In: Proceedings of the 17th Annual Meeting of ISMRM, Hawaii, USA, 2009; 2737.